SDSS-V focal plane robot positioning metrology

C. Jurgenson[a], M. Engelman[a], R. Pogge[a], T. O'Brien[a], D. Pappalardo[a], N. Clawson[a], M. Derwnent[a], C. Brandon[a], J. Mason[a], J. Brady[a], and J. Shover[a]

[a]The Ohio State University, Department of Astronomy, 140 West 18th Avenue, Columbus, OH, USA 43210-1173

ABSTRACT

The Sloan Digital Sky Survey V (SDSS-V) is an all-sky spectroscopic survey of ≥ 6 million objects, designed to decode the history of the Milky Way, reveal the inner workings of stars, investigate the origin of solar systems, and track the growth of supermassive black holes across the Universe.[1] The robotic Focal Plane System (FPS)[2] will carry 500 robots each with three fibers for science and metrology. The science fibers feed the BOSS[3] and APOGEE[4] spectrographs, while the metrology fibers are back illuminated to aid in robot positioning. Blind initial x/y positional precision of the robots is expected to be better than 50μm. The robots must position the fibers to better than 5μm in order to meet the science requirements. The FPS fiber viewing camera (FVC) consists of optomechanical components that look back through the telescope optics at light from back-lit fiducial and metrology fibers to measure the positions of the robots in the telescope focal plane. The FVC takes an image of the robots in the telescope focal plane, measures their positions to an accuracy of better than 3μm, and then feeds back error commands to the robot control system to meet the 5μm positional requirement. This paper details the optomechanical design, and initial results of an engineering run on the duPont telescope.

Keywords: SDSS-V, robot positioning, BOSS, APOGEE, Apache Point Observatory, Las Campanas Observatory, Sloan Telescope, duPont Telescope

1. INTRODUCTION

The function of the fiber viewing camera (FVC) is to provide positional information of the 500 fiber robots in the telescope focal plane. Initial x/y positional precision of the robots is required to be less than 50μm, with the FVC assisted precision to be less than 5μm. The FVC is designed to take an image of the telescope focal plane, and measure the fiber positions to an accuracy of 3μm RMS. There are approximately 70 fiber illuminated fiducials (FIF) located in the focal plane that are used as positional references to the fiber robots that are also imaged with the FVC. In designing the FVC optical system, we had to perform a thorough ray-trace analysis of the two telescopes, in particular examining the interaction of the FVC light paths with the existing telescope baffles and other features on the telescope (e.g., corrector lens mounts, edge masks on secondary mirrors, etc.) that could block rays from reaching the FVC CCD detector and compromising our ability to image the entire focal plane because of vignetting at comparable sensitivity to the light output from the fiducials and positioner metrology fibers.

2. OPTICAL DESIGN PARAMETERS

The chosen CCD camera for the FVC is the FLI ML50100. It has Kodak KAF50100 CCD with a 6132 x 8176 format, and 6μm pixel pitch. The outer ring of the FPS which contains the guide field acquisition cameras (GFA), as well as additional FIFs, extends out to a diameter of 666.4mm. This extent must be reimaged within the shortest dimension of the CCD, which is 36.8mm. A demagnification of 20 will map that 666.4mm on to 33.32mm, or 5,553 pixels resulting in 120μm per pixel sampling. Figure 1 below is a schematic showing the focal plane system layout. Blue dots are the fixed fiducials, and the red (BOSS only) and grey (BOSS + APOGEE) shaded areas represent the robot patrol fields.

jurgenson.3@osu.edu, Telephone: 1 614 688 3154, astronomy.osu.edu

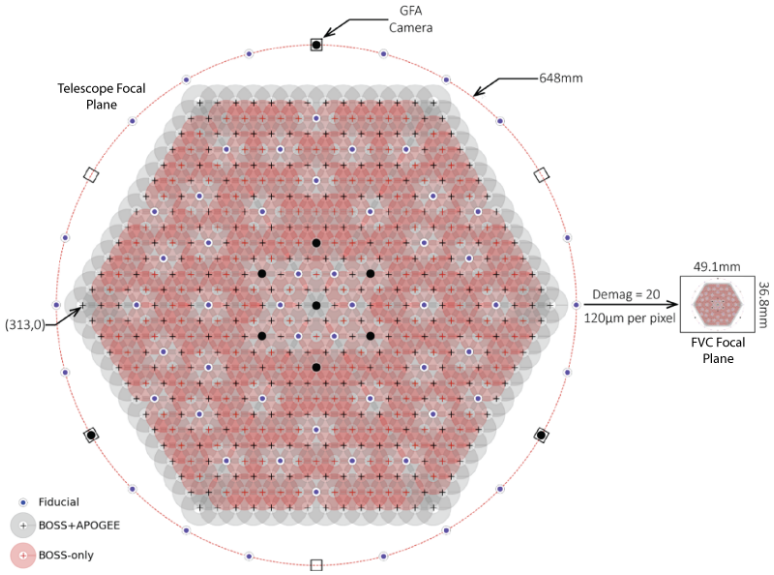

Figure 1. The telescope focal plane is reimaged on the FVC focal plane with a demagnification of 20. This results in a plate-scale of 120μm per pixel on the FVC CCD. Blue dots represent the locations of the reference position fiducials. While the grey (BOSS + APOGEE) and red (BOSS-only) shaded areas represent the robot patrol fields.

For design, analysis, and optimization of the FVC optical system, rays from seventy field points are traced from the telescope focal plane to the FVC focal plane. Sixty of these points are represent the locations of the FIFs. An additional ten were added to include a center field point at (0,0) for layout and analysis purposes. This evenly breaks the optical model into seven configurations with ten field points in each configuration. Figure 2 illustrate how these are broken up in relation to the FPS layout. Apart from the add-on fields, that includes the origin, all other field points are divided up into sextants. The colors in the figure match those in the Zemax model figures and analysis.

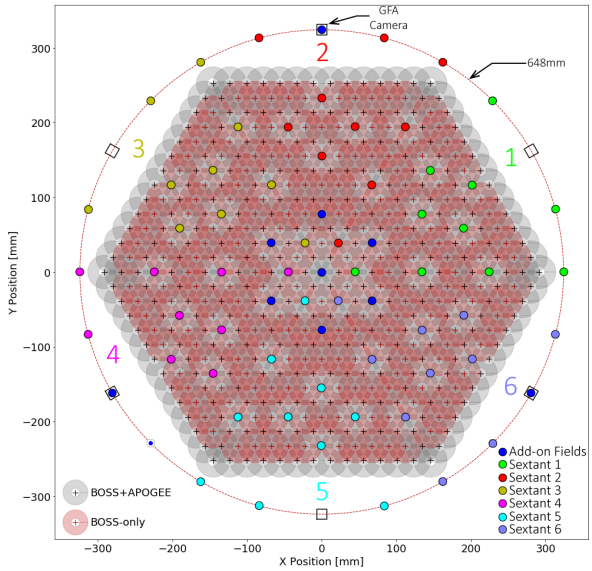

Figure 2. Zemax field points in the telescope focal plane overlaid on the FPS schematic. Fixed fiducials are color coded with sextant. These colors match those that are in the model figures and analysis.

3. SLOAN 2.5-METER FVC OPTOMECHANICAL DESIGN

3.1 FVC To Sloan Telescope Installation Location

There is currently no existing infrastructure on the Sloan 2.5-meter telescope to tap into for mounting the FVC. Figure 3 shows two profile views of the telescope. There are four regions above the primary support structure (PSS) that clear the other telescope support structures (two are shaded red in the figure below). One of these locations has been chosen for mounting the FVC components on the PSS.

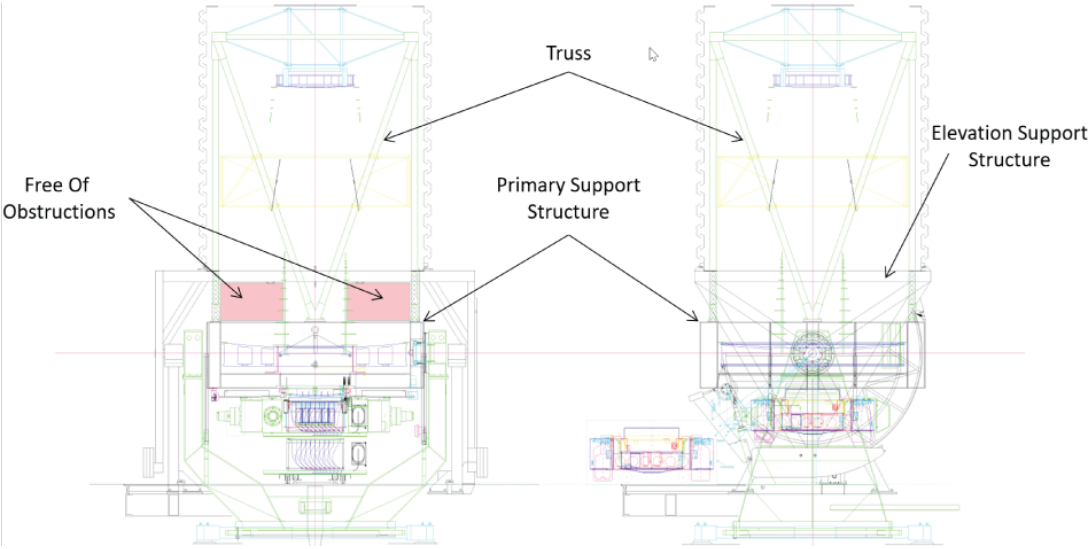

Figure 3. Two profile views of the Sloan telescope. There are four regions (two shaded in red above) that are free from obstructions where the FVC optical feed could be mounted. One of these locations has been selected.

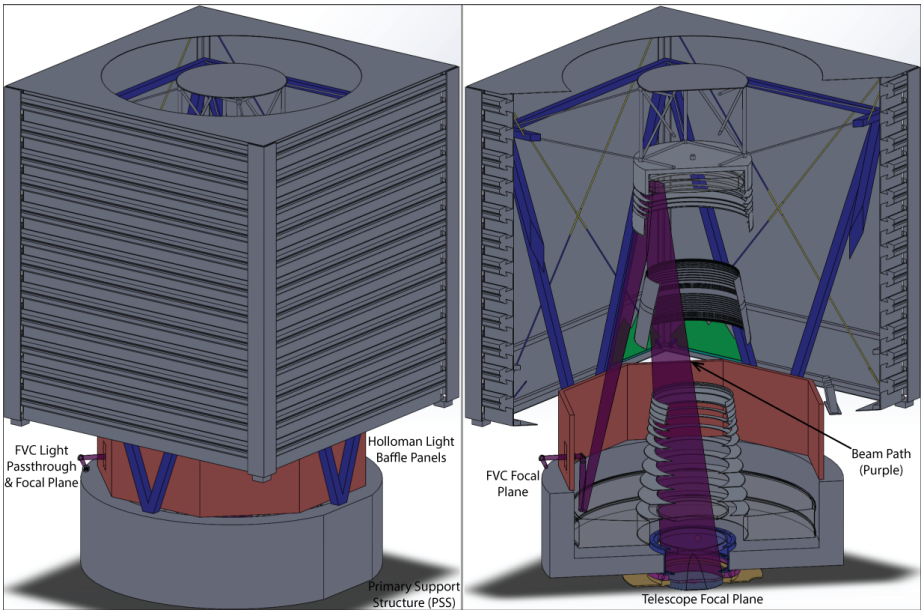

Figure 4. The Solidworks model used for determining the FVC optical layout. Left: There are eight Holloman light baffle panels that are fixed to the PSS. One of these will be replaced with a panel that allows light and the FVC optomechanics to pass through it. Right: The light path (in purple) traverses from the telescope focal plane to the FVC focal plane.

Figure 4 shows two views of the Solidworks model used to determine the optical layout of the Sloan FVC. There are a series of removable panels that are fixed to the top of the PSS. These "Holloman" light baffles, block light from the Holloman Air Force Base which sits at the base of the Sacramento Mountains, which the Sloan 2.5-meter overlooks. The plan is to remove one of the existing panels and replace it with one that has an optomechanical pass-through in it for the FVC components. The left panel of Figure 4 shows the FVC light pass-through and focal plane. The right panel highlights the beam path from the telescope focal plane, through the telescope (in reverse) to the FVC focal plane.

3.2 Optical Design & Analysis

The optical model of the Sloan 2.5-meter and FVC is shown in Figure 5.A subset of rays originate from seventy field points in the telescope focal plane with numerical apertures of 0.22 (same as fibers). They diverge through the 3-element corrector,[?] up to M2, back down to M1 where they are collimated before passing through a bandpass filter and intercepted by the FVC pick-off mirror. In this system the pick-off mirror is defined as the stop, so only rays that intersect that surface are traced. The filter is the Chroma ZET642/20X, 642nm with a 20nm bandwidth.

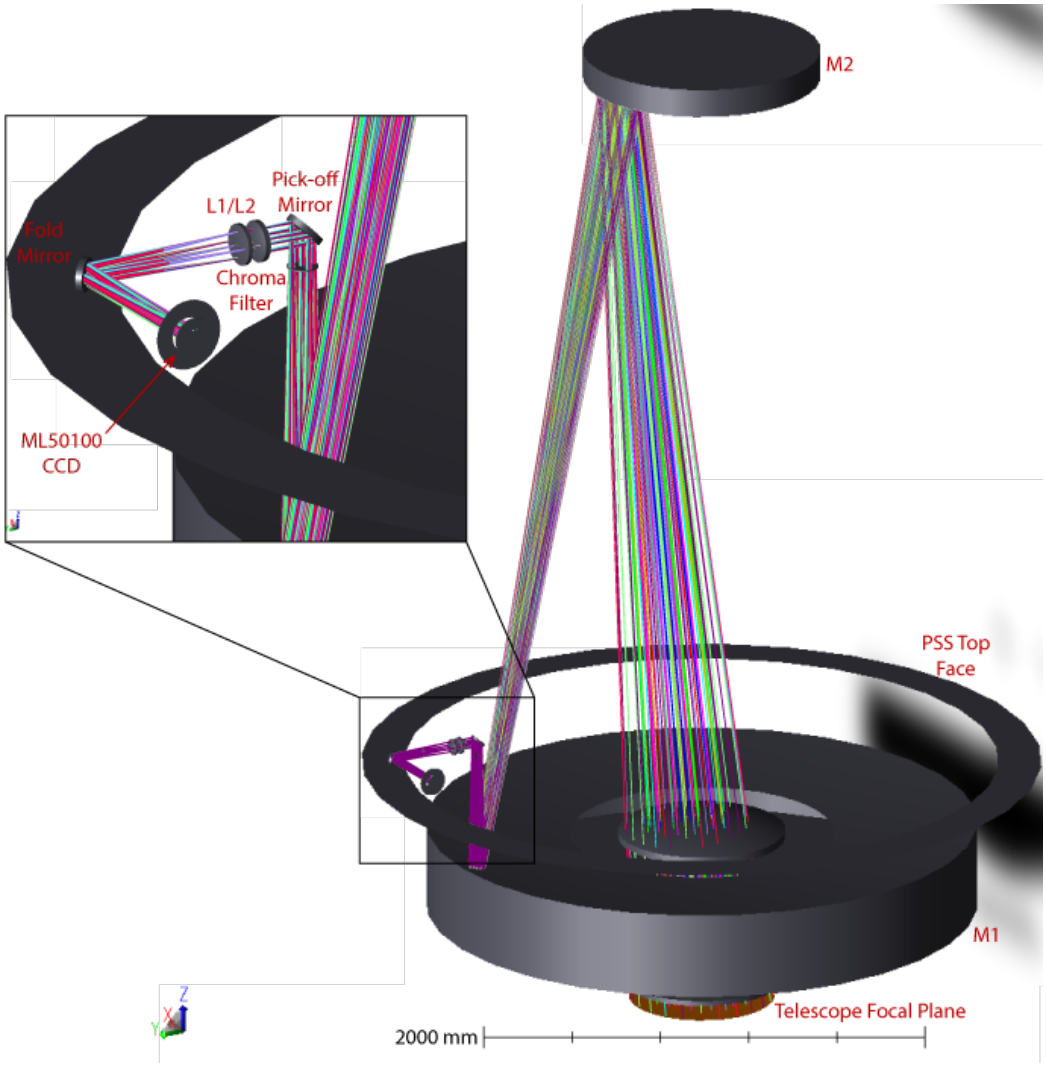

Figure 5. The optical layout of the Sloan 2.5-meter telescope with the FVC. For the model, seventy sources are placed in the telescope focal plane, and a subset of rays reverse raytraced through the telescope to the FVC optical train.

In practice light projected into the telescope from the fibers in the telescope focal will completely illuminate M2. By selecting the pick-off mirror as the stop and using the Zemax vignetting factors, only the rays that are collected by the stop are traced. Following the pick-off mirror there are two meniscus lenses made of the same material (Ohara S-NPH2). S-NPH2 is a high index (1.92) low Abbe number (18.9) glass with high transmission beyond 550nm.

After the focusing elements, the beam is folded horizontally and directed toward the FLI ML50100 CCD camera. Not shown in Figure 5 are four aperture stops placed in the beam path. One in front of the Chroma filter, one either side of the L1/L2 grouping, and a final one in front of the fold mirror. These function to not only reduce scattered light, but out of field light that can enter the system from outside the optic clear apertures. Figure 6 is a footprint diagram of the reimaged telescope focal plane sources on the FVC focal plane. To achieve the required demagnification of 20, results in a camera focal length of 628.8mm. This results in a plate-scale of 120μm per pixel. The depth-of-focus of the system is of order +/-150μm.

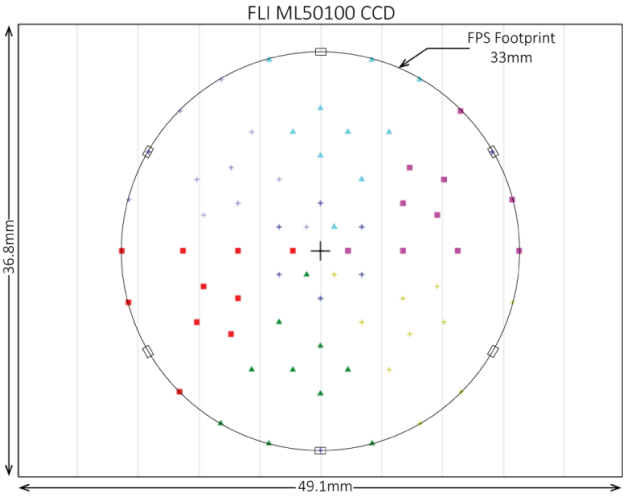

Figure 6. The Zemax footprint diagram of the reimaged telescope focal plane at the FVC focal plane. The demagnification of 20 results in a plate-scale of 120µμm per pixel.

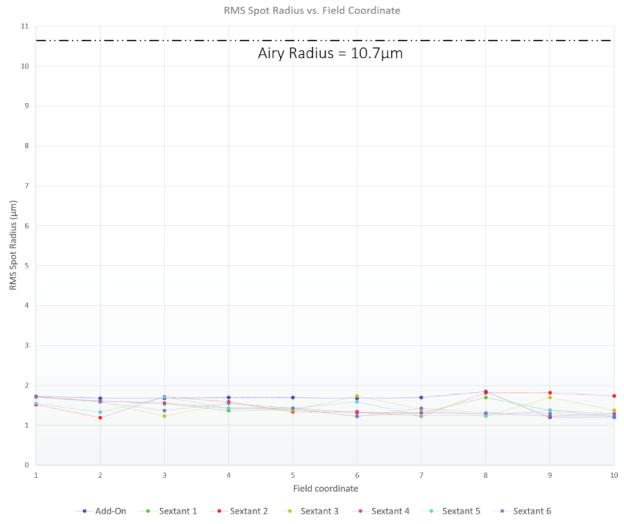

Figure 7. RMS spot radius for all fields is less than 2μm. The system is diffraction limited since the geometric radii are comparatively small relative to the Airy radius of 10.7μm.

The RMS spot radius is shown in Figure 7. It is predicted to be less than 2µm for all field points in the focal plane. The Airy radius, represented by the dashed black line at the top of the plot is 10.7μm. The geometric radii are comparatively small relative to the Airy radius, and therefore the system can be considered to be diffraction limited. Figure 8 is a plot of the diffraction ensquared energy for the 10 field points in the add-on configuration. The Airy radius is the black dashed line at 10.7μm. The Airy disc would fall within a 4x4 pixel box on the CCD.

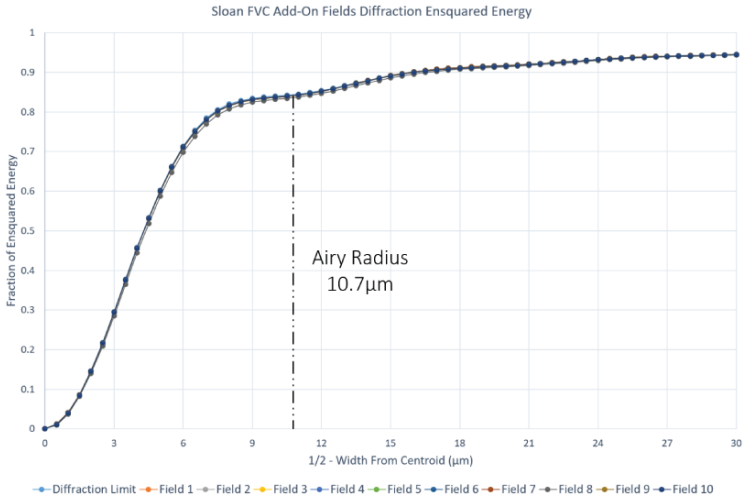

Figure 8. The diffraction ensquared energy for the 10 field points in the add-on configuration (Figure 2). The Airy disc falls within a 4x4 pixel box.

3.3 Sloan FVC Mechanical Design

At Apache Point, the FVC mechanically interfaces with the PSS via a steel supporting column (Figure 9). This column also serves as the adjustment mechanism for the FVC to ensure that it is aligned to the telescope axis, and it has three open degrees of rotation for this adjustment. Three spring loaded shoulder screws hold the FVC in place atop the column while ball tip adjustment screws allow for tip-tilt adjustment. The third rotation comes from the rotation of the column itself within its base plate. On top of this column, the FVC is epoxied inside a "birdhouse" part that is mounted to the plate supported by the adjustment screws.

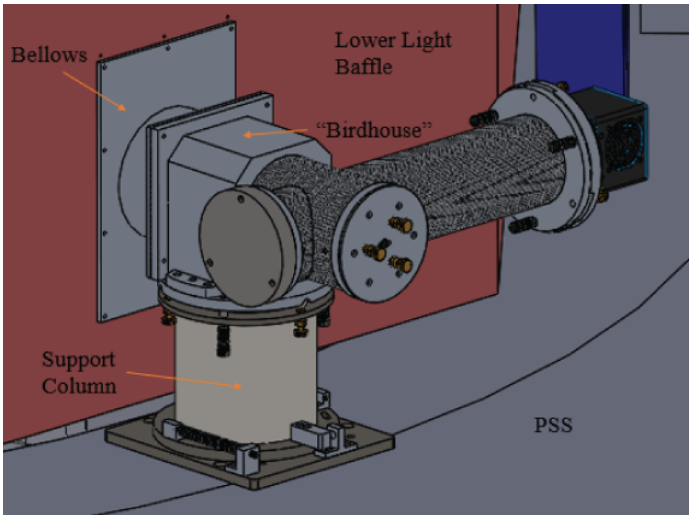

Figure 9. The Sloan FVC mechanical interface to the telescope and overall mechanical design.

The pick-off mirror protrudes through a cutout in one of the Holloman light baffles above M1. This cutout is covered up when in use by a set of accordion bellows to keep extraneous light from entering the telescope. The two ends of the bellows are mounted to a bolt pattern around the cutout in the baffle and the part that holds the FVC on top of the column. The two materials used for the main FVC assembly (defined as only the parts that include and enclose the optical path) are aluminum and carbon fiber. A two-part epoxy was used to join the materials where they meet. Another epoxy was used on the shoulder joint where the two carbon fiber tubes meet.

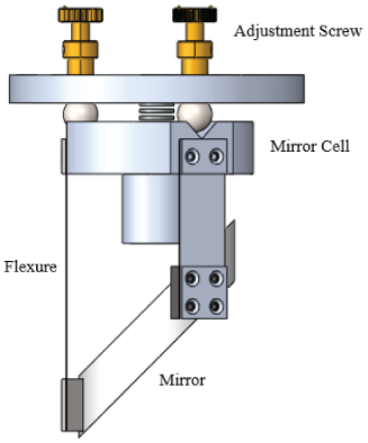

Figure 10. The optomechanical adjustment mechanism of the pick-off mirror used for internal alignment of the FVC optical axis.

The pick-off mirror is held in place with aluminum and stainless steel flexures attached to an aluminum cell, which in turn was held against three adjustment screws mounted in the overall mirror enclosure (10). The fold mirror is supported in the same manner, just in a horizontal orientation instead of vertical. The flexure material, thickness, and length were optimized using a combination of finite element analysis (FEA) and MATLAB to limit image motion on the CCD and mirror distortion that could occur due to thermal effects over the operating temperature range of -20C to +20C. Three adjustment screws were included in the elliptical mirror subassembly to a) provide mechanical stability for the mirror and b) to have tip, tilt, and piston adjustment available to calibrate the internal alignment of the FVC. The same mechanical design and analysis also applies to the fold mirror.

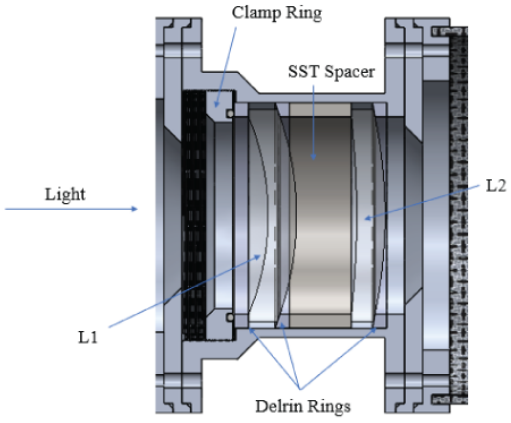

Figure 11. The lens barrel for the FVC doublet.

The lens doublet for the FVC was secured in an aluminum "barrel" enclosure. This is shown in Figure 11 above. Inside, the lenses were held in place by a combination of Delrin plastic and stainless steel spacers as well as a clamping ring. The Delrin rings were used to support the backs of each lens and were machined to be tangent to back lens surface. One flat Delrin ring was also used to bear the load of the clamp ring, which provides a clamping force to hold the stack of lenses and spacers firmly in place. The stainless steel spacer was used to maintain the prescribed distance between the lenses. Stainless steel was used in this case instead of Delrin because of a lower linear coefficient of thermal expansion. This was important to maintain the spacing between L1 and L2 over the operating temperature range. Between the lenses and inner wall of the barrel, bits of Viton O-ring were inserted to act as springs to keep the lenses concentric.

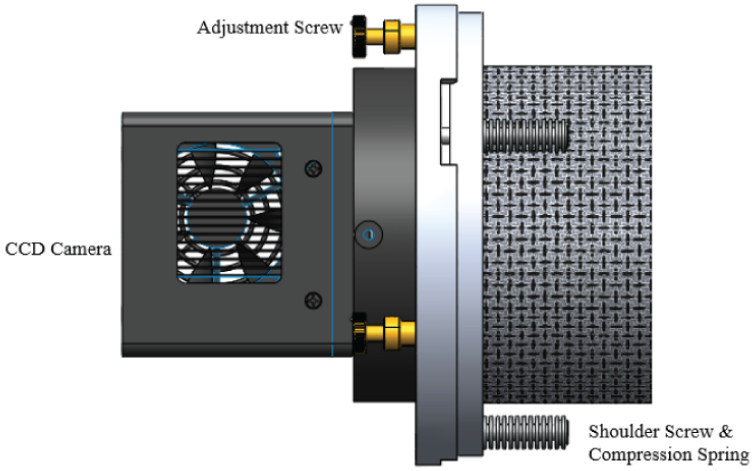

Figure 12. The CCD mount design to the FVC carbon fiber tube structure. This design provides tip-tilt adjustment as well as focus.

Placing the CCD detector within the depth of focus margin was a critical requirement for the FVC. To ensure that this was possible, a mechanism for adjusting the position of the detector was included. Three spring-loaded shoulder screws held the camera against the back of the carbon fiber tube, while three ball-tip adjustment screws are actuated by hand to induce a piston motion of the detector. It was designed such that there would nominally be two millimeters of travel possible in each direction. The mechanical design of the CCD mount to the FVC carbon fiber barrel is shown in Figure 12.

4. DU PONT 2.5 METER FVC OPTOMECHANICAL DESIGN

4.1 Du Pont To FVC Installation Location

The du Pont telescope has two declination axis ports (west and east) with mounting interfaces available. Figure 9 shows two views of a simplified du Pont Solidworks model with the FVC optical train. It was decided to install it on the west part due to the existence of encoding hardware on the east port. As part of the design process, models were created in FRED for both telescope to FVC systems to ensure that the FVC would have complete visibility of the telescope focal plane from its mounting locations through the telescope baffles. For Sloan the baffles do not obstruct the FVC view, however, as can be seen in Figure 13, this is not the case for du Pont. As a result, the du Pont baffles were redesigned by the Carnegie Observatories. This analysis is discussed more in Section 4.4.

4.2 du Pont Focal Plane Curvature

SDSS-V will expand the operational wavelength of the du Pont SDSS-IV project by extending it down into the visible. du Pont SDSS-IV operates solely with APOGEE spectrograph (1.51 to 1.7µm), while Sloan currently has APOGEE, and two BOSS spectrographs (0.36 to 0.96µm). One of the BOSS spectrographs will be installed

on du Pont extending its operational wavelength range into the visible. Measurements of the du Pont focal plane were made to reference the fiber positions for SDSS-IV,[5] however, there was a question of how it would perform extending across the entire visible to near-IR wavelengths. Using the Zemax fitted model of the telescope based on the measurements made for APOGEE, and investigation was done to determine optimal geometric spot size and telecentricity across the entire SDSS-V wavelength range.

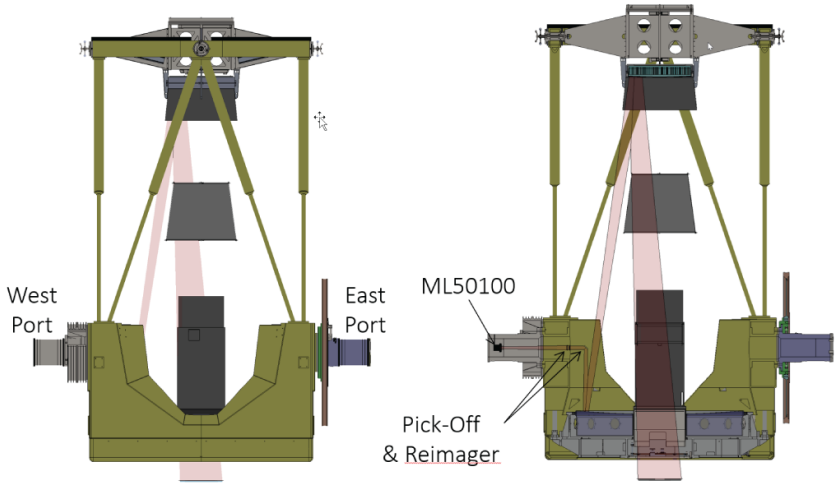

Figure 13. A simplified version of the du Pont telescope Solidworks model with the FVC system. The west port will be used to mount the FVC. As can be seen in the right panel, the red FVC beam is blocked by the current baffle system. It has since been redesigned and replaced.

Figure 14 are the spot diagrams for the BOSS (left panel) and APOGEEE (right panel) wavelengths for nine du Pont field angles for the telescope in its SDSS-IV configuration. Both panels show the spots relative to their respective fiber core diameters (BOSS 180μm/APOGEE 120μm). If the SDSS-IV telescope configuration (corrector and focal plane position) is kept in place, but the shape of the focal plane is allowed to depart from a sphere, the telecentricity can be improved. Figure 15 plots the BOSS and APOGEE telecentricity as a function of field angle for a spherical (grey) and aspheric (blue/red) focal plane curvature. It is possible to improve the telecentricity, and bring more balance between the BOSS and APOGEE geometric spot sizes, but that would involve not only a curvature change, but a change in telescope configuration.

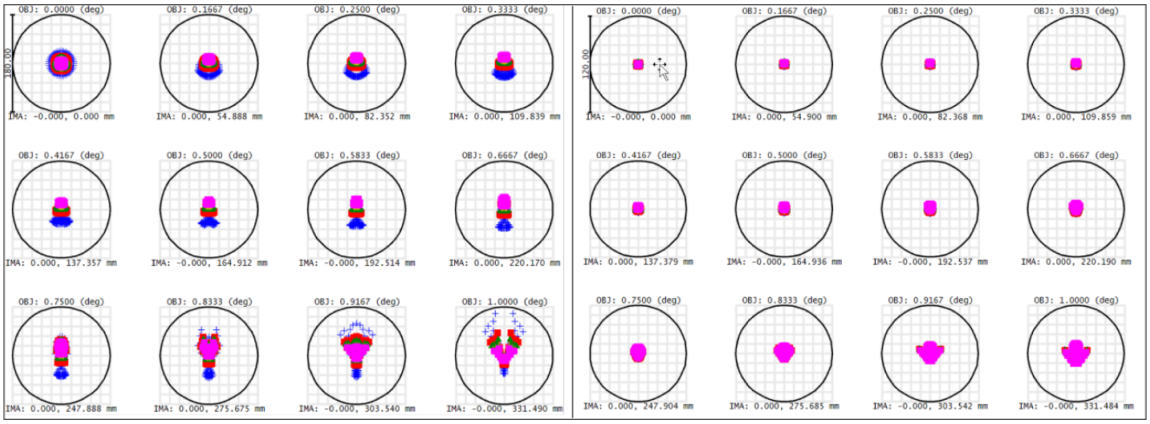

Figure 14. *Left Panel*: Spot diagrams for the BOSS wavelengths across the du Pont field of view. The circle represents the 180μm fiber core diameter. *Right Panel*: Spot diagrams for the APOGEE wavelengths. The circle represents the current 120μm fiber core diameter.

The below equation describes the focal plane curvature, and the 2nd order aspheric term for the improvement in telecentricity in Figure 15 below.

$$z(r) = \frac{c^2 r^2}{\sqrt{1 - c^2 r^2}} + \alpha_1 r^2 \tag{1}$$

where c is the focal plane radius of curvature (1/8800mm) at the vertex, r is the radial coordinate, and $\alpha_1 = 1.2336E^{-6}$.

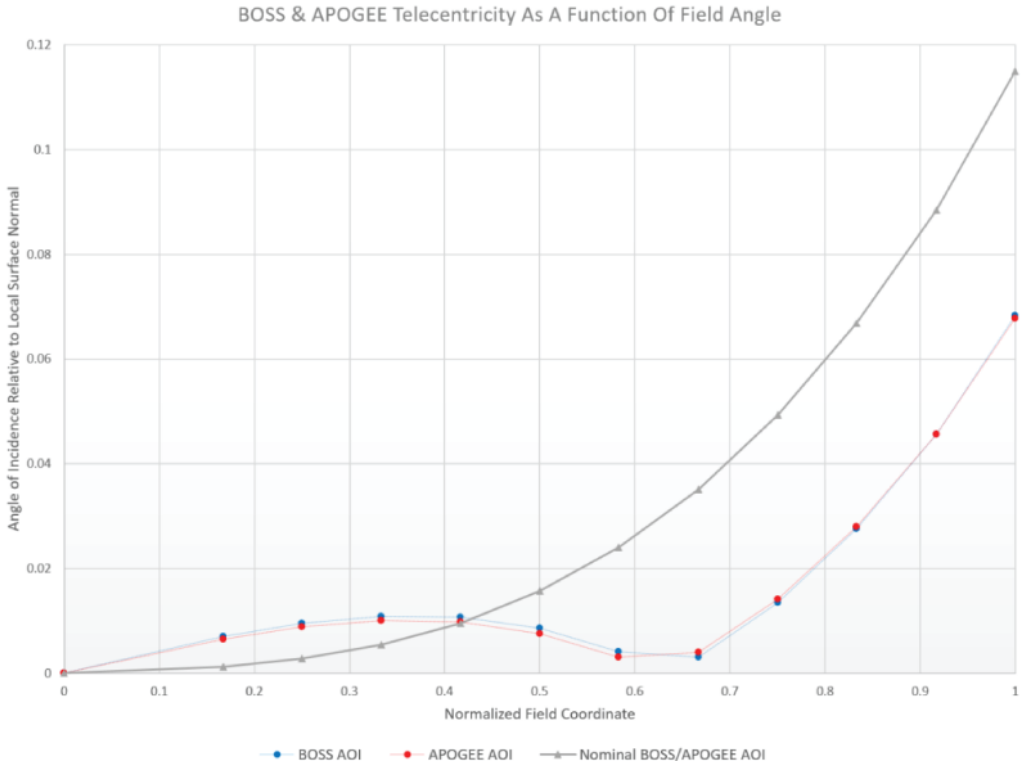

Figure 15. BOSS and APOGEE telecentricity as a function of field angle. Grey line plots telecentricity with current focal plane shape, and the red and blue plot telecentricity with the aspheric shape described above.

4.3 du Pont FVC optical design & Analysis

In practice light projected into the telescope from the fibers in the telescope focal will completely illuminate M2. By selecting the pick-off mirror as the stop and using the Zemax vignetting factors, only the rays that are collected by the stop are traced. Following the pick-off mirror there are two meniscus lenses made of the same material (Ohara S-NPH2). S-NPH2 is a high index (1.92) low Abbe number (18.9) glass with high transmission beyond 550nm.

The FVC optical raytrace is shown in Figure 16. Rays originate from seventy field points in the telescope focal plane with numerical apertures of 0.22. They diverge through the corrector to M2, and M1 where they are collimated. A pick-off mirror above M1 directs the rays into the FVC optical train. In this system, the pick-off mirror is defined as the stop, so only rays that intersect that surface are traced. In practice, the fiducials will completely illuminate M2. In front of the pick-off mirror is the same Chroma 640nm filter as for Sloan. After the pick-off mirror there are two meniscus lenses made of the same Ohara material, S-NPH2. Figure 13 is a footprint diagram of the reimaged telescope focal plane in the FVC focal plane. To achieve the demagnification of 20, requires a camera focal length of 943.3mm. This results in a plate-scale of 120μm per pixel. The depth-of-focus of the system is of order +/-460μm.

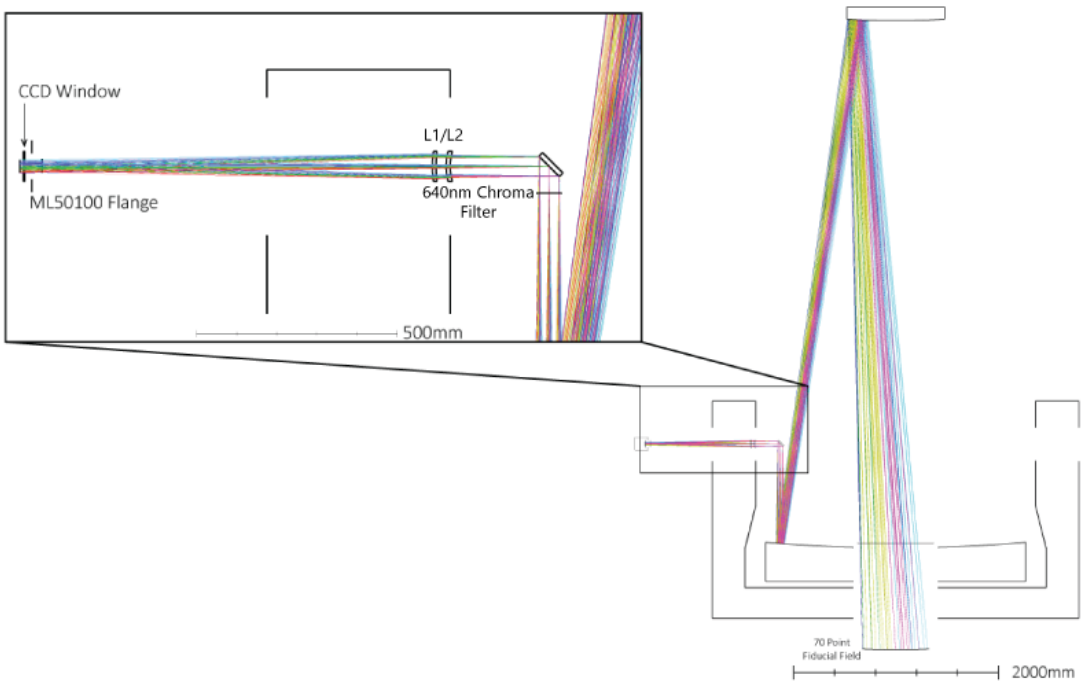

Figure 16. The FVC optical raytrace. Rays originate in the telescope focal plane with numerical apertures of 0.22, diverge through the corrector to M2, then to M1 where the beams are collimated, and is then routed through the FVC optical train via a pick-off mirror.

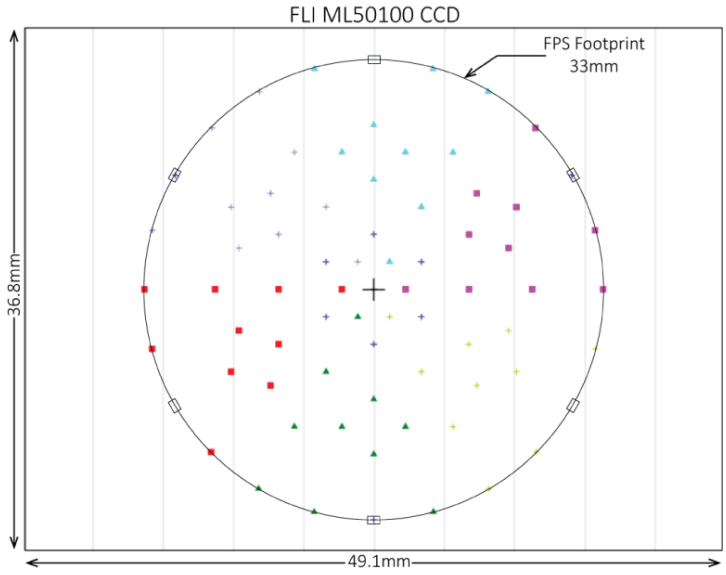

Figure 17. The Zemax footprint diagram of the reimaged telescope focal plane at the FVC focal plane. The demagnification is 20, resulting in a plate-scale of 120µm per pixel.

In Figure 18 the RMS spot radius is shown to be less than 1m for all field points in the focal plane. The Airy radius of 15.4μm is the dashed black line at the top of the plot. The geometric radii are comparatively small relative to the Airy radius, and therefore the system can be considered to be diffraction limited. Figure 19 is a plot of the diffraction ensquared energy for the 10 field points in the add-on configuration. The Airy radius is the black dashed line at 15.4μm. The Airy disc would fall within a 6x6 pixel box on the CCD.

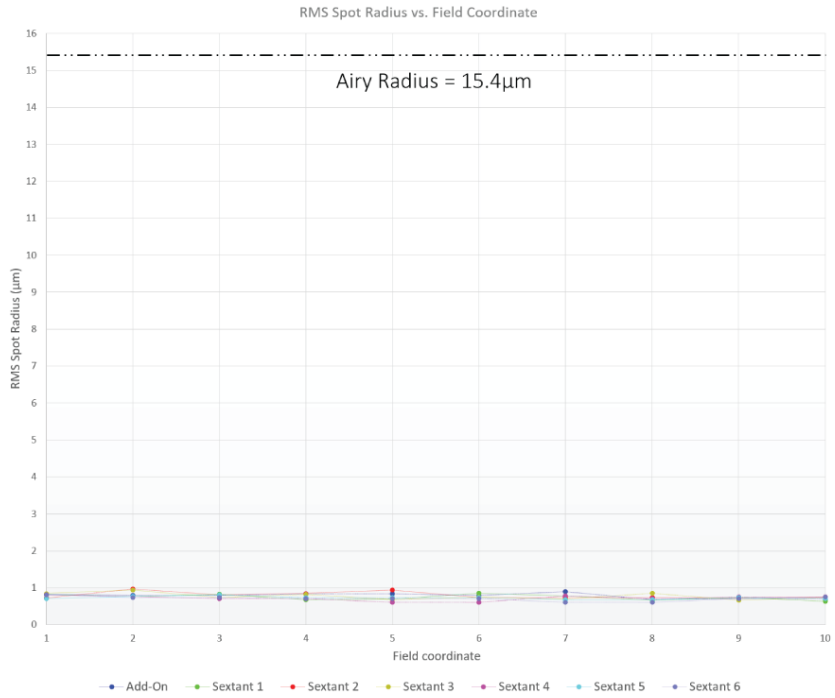

Figure 18. RMS spot radius for all of the fields is less than 1μm. The geometric radii are comparatively small relative to the Airy radius of 15.4μm, therefore the system can be considered to be diffraction limited.

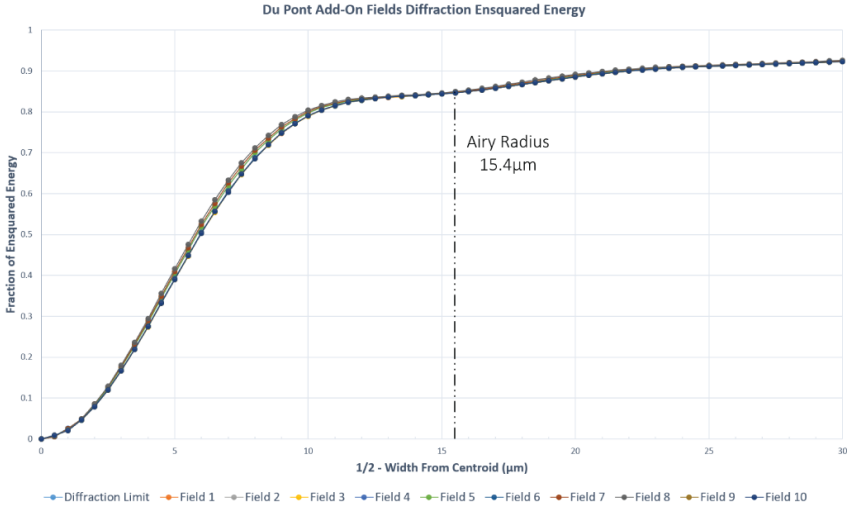

Figure 19. The diffraction ensquared energy for the 10 field points in the add-on configuration. The Airy disc falls within a 6x6 pixel box.

4.4 du Pont FVC vignetting analysis

A model was constructed in FRED to conduct a reverse raytrace from the FVC focal plane to the du Pont telescope focal plane. The model combined both the Zemax optical prescription and the Solidworks mechanical model shown in Figure 13. This was done to determine whether or not the entire telescope focal plane is visible to the FVC focal plane. A source was placed in the FVC focal plane, and rays are randomly emitted into angular directions toward the pick-off mirror. No scattering is accounted for and all optics are treated as ideally reflective or transmissive. All other mechanical surfaces are 100% absorbers.

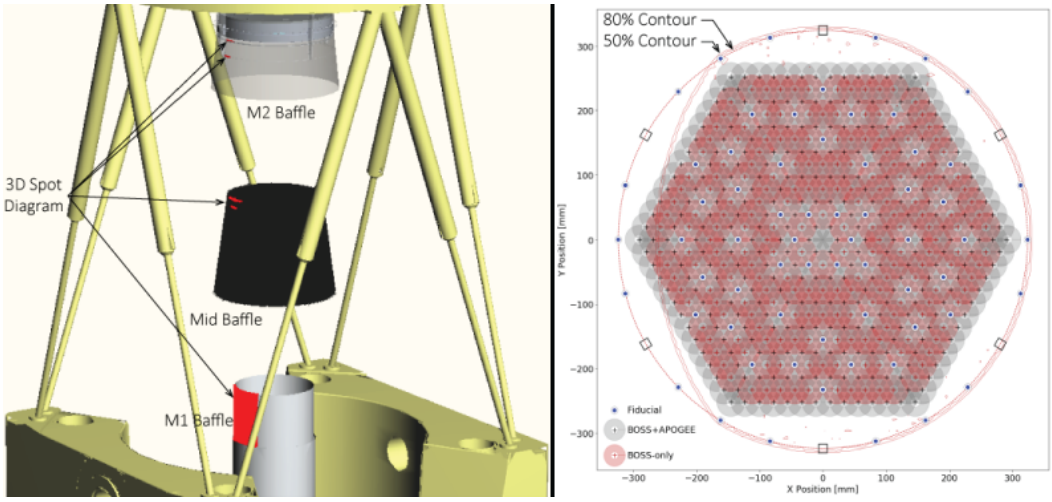

Figure 20. *Left*: This is a section of the Du Pont FRED model showing the 3D spot diagram. These are ray intersection points showing the causing the vignetting in the reverse raytrace. *Right*: Is a contour plot of the irradiance in the telescope focal plane plotted over the FPS schematic. The FVC has zero visibility of the telescope focal plane beyond the 50% contour.

The left panel in Figure 20 is the 3D spot diagram showing ray intersections from the FVC focal plane source. These are rays that do not make it to the telescope focal plane, and illustrate which parts of the telescope focal plane are not visible to the FVC camera. Vignetting occurs at the M2 stop, M2 baffle, mid baffle, and M1 baffle. The right panel in Figure 20 is a contour plot of the resulting irradiance in the telescope focal plane, plotted over the FPS schematic. Beyond the 50contour the FVC has zero visibility of the telescope focal plane. In order for the FVC to see the entire telescope focal plane at this location, the baffle system needs to be modified. The biggest offender is the M1 baffle. As a result, a new baffle system for du Pont was designed and fabricated for the SDSS-V project.

4.5 du Pont FVC Mechanical Design

On the du Pont telescope, the FVC is located inside the west port on the declination axis. It is mounted inside the port by means of a large steel tube that interfaces with the 12-bolt pattern on the trunnion of the telescope. At the end of the tube is a "horseshoe" flange that mates via a bolted connection with a flange that is epoxied on the carbon fiber tube of the main FVC assembly as shown in Figure 21.

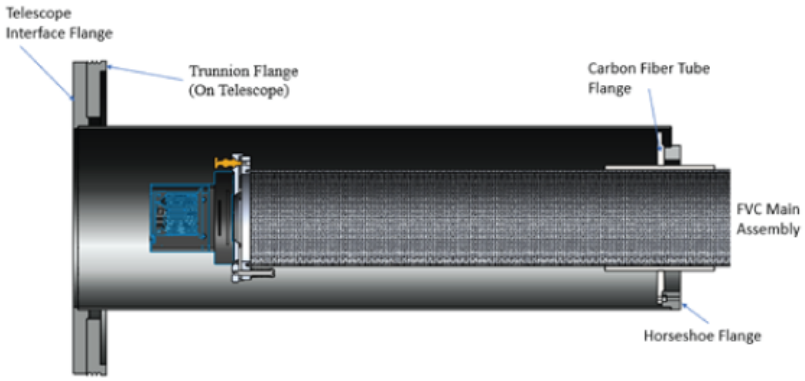

Figure 21. The overall mechanical design of the du Pont FVC showing the telescope interface.

When installing, the large tube is mounted inside the port first, then the FVC assembly is slid into the tube until the flange on the carbon fiber meets the horseshoe flange at the end of the interface tube, and finally the

two are bolted together. The location of the flange on the carbon fiber was chosen to be at the center of gravity of the main FVC assembly such that there is minimal gravitational torque acting on the FVC (when the telescope is at its zero-hour position).

The pick-off mirror for the du Pont FVC is the same as the pick-off and fold mirrors in the Sloan FVC. This is shown in Figure 22. It is held in place with aluminum and stainless steel flexures attached to an aluminum cell, which in turn was held against three adjustment screws mounted in the overall mirror enclosure. The fold mirror is supported in the same manner, just in a horizontal orientation instead of vertical. The flexure material, thickness, and length were optimized using a combination of finite element analysis (FEA) and MATLAB to limit image motion on the CCD and mirror distortion that could occur due to thermal effects over the operating temperature range of -20C to +20C. Three adjustment screws were included in the elliptical mirror subassembly to a) provide mechanical stability for the mirror and b) to have tip, tilt, and piston adjustment available to calibrate the internal alignment of the FVC.

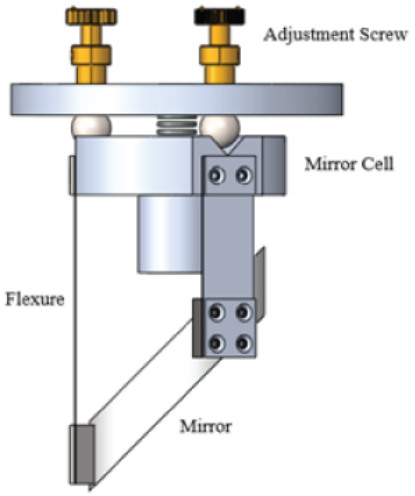

Figure 22. The optomechanical adjustment mechanism of the pick-off mirror used for internal alignment of the FVC optical axis. Design is identical to that for Sloan.

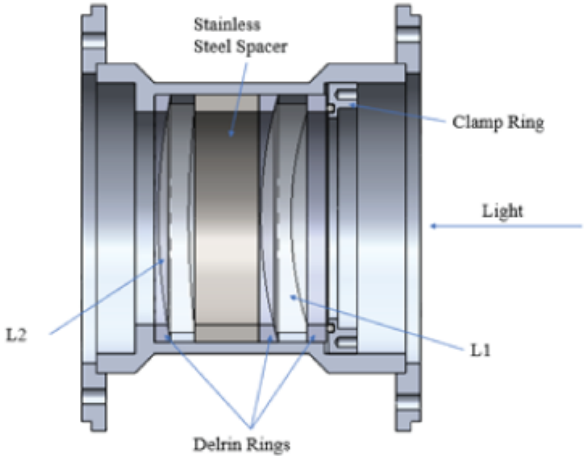

Figure 23. The optomechanical design for the du Pont lens barrel.

The lens doublet for the FVC are secured in an aluminum "barrel" enclosure. Inside, the lenses are held in place by a combination of Delrin plastic and stainless steel spacers as well as a clamping ring. The Delrin rings

were used to support the backs of each lens and were machined to be tangent to back lens surface. One flat Delrin ring was also used to bear the load of the clamp ring, which provides a clamping force to hold the stack of lenses and spacers firmly in place. The stainless steel spacer was used to maintain the prescribed distance between the lenses. Stainless steel was used in this case instead of Delrin because of a lower linear coefficient of thermal expansion. This was important to maintain the spacing between L1 and L2 over the operating temperature range. Between the lenses and inner wall of the barrel, bits of Viton O-ring were inserted to act as springs to keep the lenses concentric.

An identical CCD camera and focus adjustment mechanism were used for the du Pont FVC as for the Sloan FVC. Three spring-loaded shoulder screws held the camera against the back of the carbon fiber tube, while three ball-tip adjustment screws are actuated by hand to induce a piston motion of the detector. It was designed such that there would nominally be two millimeters of travel possible in each direction. This is shown is Figure 24.

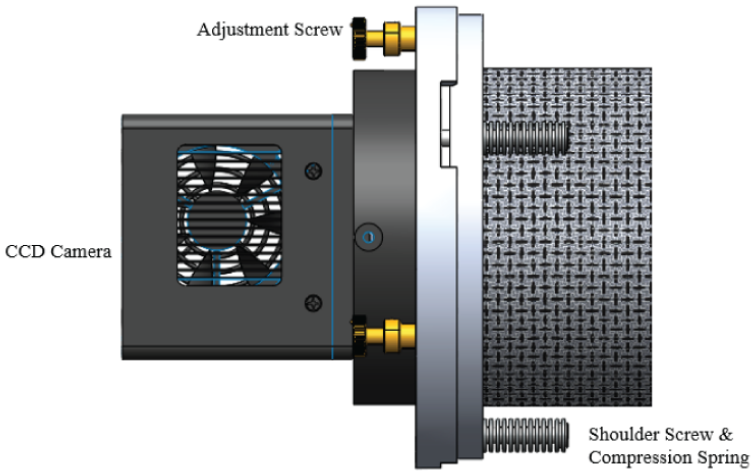

Figure 24. The CCD mount design to the FVC carbon fiber tube structure. This design provides tip-tilt adjustment as well as focus.

The need for an athermalized mechanical assembly remains the same for the du Pont FVC as the Sloan FVC. Carbon fiber was used around the greatest part of the optical path length as was feasible to limit the amount of thermal expansion and contraction over the operating temperature range. Similar to the Sloan FVC, a two-part epoxy was used to affix the metal-carbon fiber joints. This is shown in Figure 25.

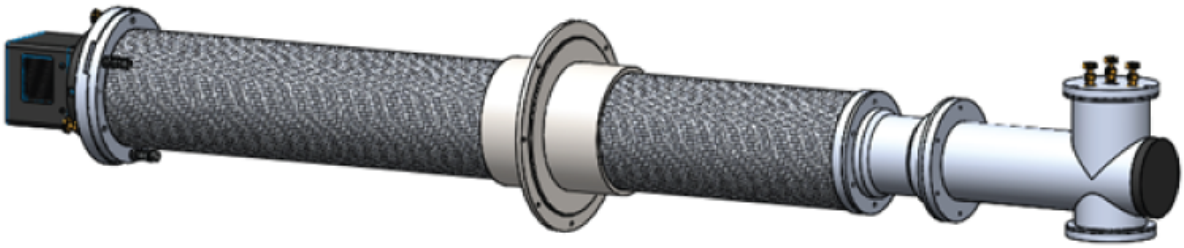

Figure 25. The carbon fiber tube design restricts the linear expansion of the assembly to remain well within the depth-of-focus of the optical system.

5. LAB AIT & DU PONT ENGINEERING RUN

5.1 Lab Assembly Integration & Verification

An engineering run for the du Pont FVC was scheduled to take place from January 28^{th} through February 2^{nd} 2020. Prior to shipment to Chile, the FVC was assembled on an optical bench for assembly, integration, and

verification (AIV) of the system as a whole. The most straight-forward way to verify the optics was to test them as a unit. The lens doublet assembly was first mounted to an optical bench. 640nm wavelength light from an integrating sphere was passed through a 10μm pinhole, collimated before being directed into the FVC by a pair of alignment mirrors. The back focal distance, depth-of-focus, and image FWHM was recorded and verified with the Zemax model.

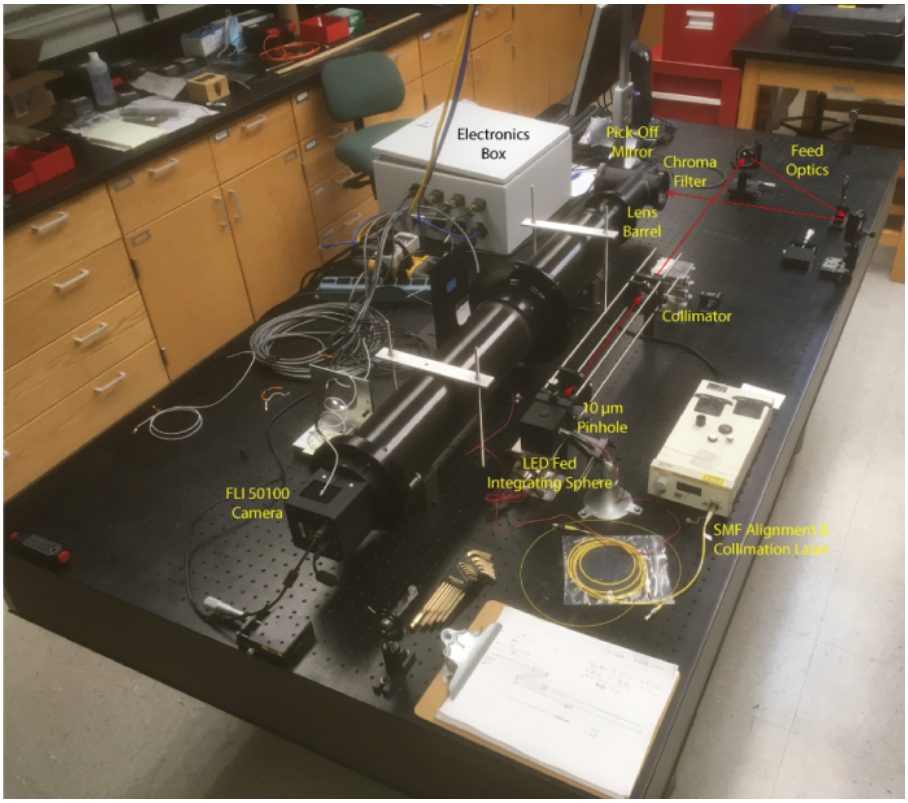

Figure 26. The assembly level verification of FVC in the OSU laboratory. 640nm laser light is fed into an integrating sphere and passed through a 10μm pinhole before being collimated and fed into the fVC. The light is then focused by the FVC doublet onto the FLI camera.

The next step was to verify system performance with the doublet mounted into the entire FVC assembly. This setup is shown in Figure 26. The first step was to verify axial alignment of the FVC optical axis to the of the beam injection optical axis. With FVC assembly mounted to the optical bench, tilt and shear errors between the two axes were removed via a pair of alignment mirrors using pinhole fiducials at either end of the FVC barrel. Once alignment was established, a back illuminated 10μm pinhole was collimated and directed into the FVC barrel. As with the stand-alone doublet setup discussed above, image quality, focus location, as well as depth-of-focus were verified with the Zemax optical model.

5.2 du Pont Engineering Run

A custom APOGEE test mask was designed and fabricated that uses 232 of the available 300 APOGEE science fibers to cover the FPS field of view with a metrology grid. The core pattern was a 184-point isometric (triangular) grid with a spacing of 40.5-mm that covers the primary field, plus an outer ring of fibers with a radius 324-mm spaced every 7.5 degrees. The science fibers were installed on this plate as if it were a plate for night-time observations, but without the usual bright/faint restrictions on fiber/plate assignments. These fibers were back illuminated by an integrating sphere outfitted with a custom interface to plug into the female gang connector on the plug-plate cartridge, taking the place of the male gang connector that attaches the long fiber bundle that connects the fibers to the slit head inside the APOGEE spectrograph.

The test plan consisted of cycling the telescope through a grid of hour angle, declination, and rotator angles and taking images of the back illuminated science fibers in the telescope focal plane. Hour angle and declination positions were determined to evenly sample the current notional SDSS-V APOGEE and BOSS survey footprints. From these footprints it was determined that the FVC will take images of the back illuminated focal plane at hour angles from -3^h to $+3^h$ in 1^h steps at declinations of 25°, 50°, and 75°. This also covers the nominal range over which we are concerned about now flexure might effect performance of the FVC. Figure 27 is an image taken by the FVC of the back illuminated fibers in the focal plane of the du Pont telescope.

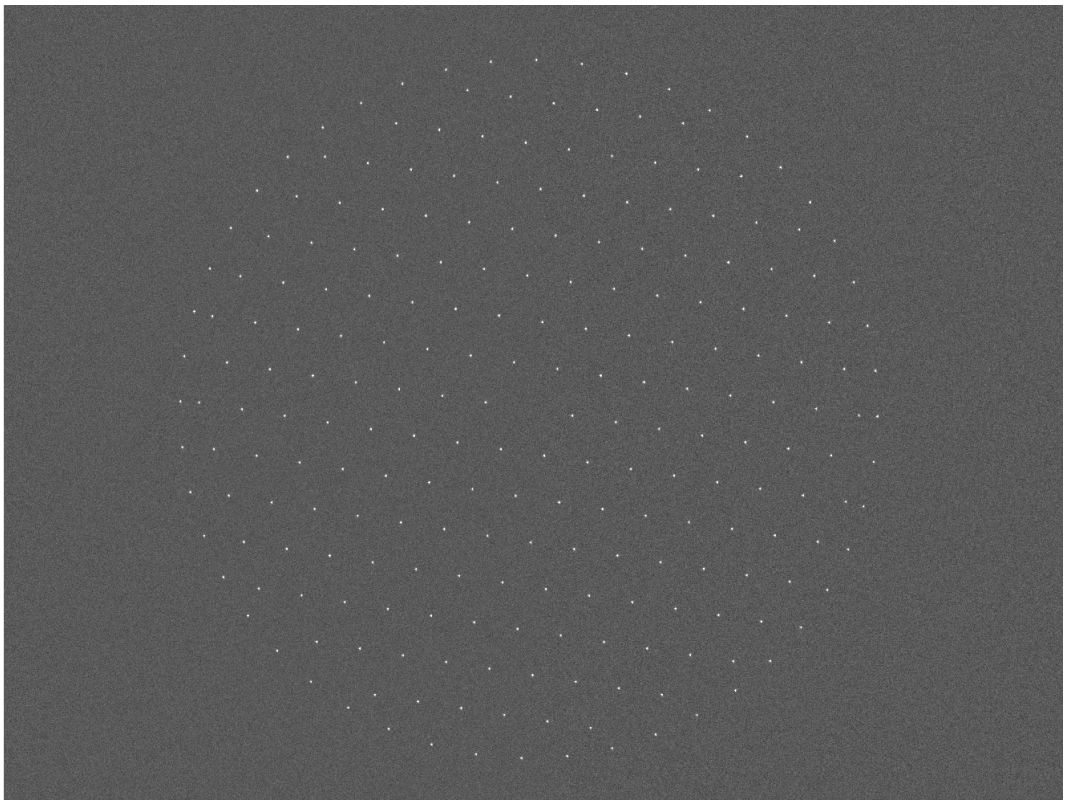

Figure 27. An image taken by the FVC of the back illuminated fibers in the telescope focal plane.

The isometric grid pattern described at the beginning of Section 5.2 is clearly seen in the figure. Individual images of the fiber tips were consistent in size with the optical models, but also consistent with one another from one field point to another. There were no adverse effects on imaging performance from the observations at different hour angle and declination positions, and flexure was minimal, few 10s of pixels maximum out of a total spot that is about 5800 pixels in diameter. However, all spots were observed to have the same asymmetric shape in the PSF wings that was determined to be the result of the FVC internal baffles not being installed. Baffles have been designed and locations identified within the FVC optical system to mitigate this problem. A followup engineering run to repeat this with the baffles and other enhancements has been postponed due to the COVID-19 shutdown of the observatory.

ACKNOWLEDGMENTS

Funding for the Sloan Digital Sky Survey V has been provided by the Alfred P. Sloan Foundation, the Heising-Simons Foundation, and the Participating Institutions. SDSS acknowledges support and resources from the Center for High-Performance Computing at the University of Utah. The SDSS web site is www.sdss5.org.

SDSS is managed by the Astrophysical Research Consortium for the Participating Institutions of the SDSS Collaboration, including the Carnegie Institution for Science, Chilean National Time Allocation Committee (CN-

TAC) ratified researchers, the Gotham Participation Group, Harvard University, The Johns Hopkins University, L'Ecole polytechnique fédérale de Lausanne (EPFL), Leibniz-Institut für Astrophysik Potsdam (AIP), Max-Planck-Institut für Astronomie (MPIA Heidelberg), Max-Planck-Institut für Extraterrestrische Physik (MPE), Nanjing University, National Astronomical Observatories of China (NAOC), New Mexico State University, The Ohio State University, Pennsylvania State University, Smithsonian Astrophysical Observatory, Space Telescope Science Institute (STScI), the Stellar Astrophysics Participation Group, Universidad Nacional Autónoma de México, University of Arizona, University of Colorado Boulder, University of Illinois at Urbana-Champaign, University of Toronto, University of Utah, University of Virginia, and Yale University.

REFERENCES

[1] Kollmeier, J. and Collaboration, "Sdss-v: Pioneering panoptic spectroscopy." arXiv, 2017, https://arxiv.org/abs/1711.03234.

[2] Pogge, R. and Collaboration, "A robotic focal plane system (fps) for the sloan digital sky survey v," *Paper number 11447-173 This conference proceedings* (2020).

[3] Smee, S. and Collaboration, "The multi-object, fiber-fed spectrographs for the sloan digital sky survey and the baryon oscillation spectroscopic survey," *AJ* **146, 32** (2013).

[4] Wilson, J. and Collaboration, "The apache point observatory galactic evolution experiment (apogee) spectrographs," *PASP* **131, 999** (2019).

[5] Blanton, M. and Collaboration, "Sloan digital sky survey iv: Mapping the milky way, nearby galaxies, and the distant universe," *AJ* **154, 28** (2017).